AUGMENTING THE PHILIPPINES' DOST-ASTI'S POTENTIAL FLOOD EXTENTS MAPPING SERVICE WITH S-BAND NOVASAR-1 IMAGES

J.B.L. C. Dumalag [1 2] *, K.L. S. Mariano [1 2], N.R. Cadiz [1 2], A.E. Retamar [1 2], J.C. Aceron [1 2], M.M. Felicen [1 2], M.C. Gelido [1 2]

[1] Synthetic Aperture Radar and Automatic Identification System for Innovative Terrestrial Monitoring and Maritime Surveillance (SAR w/AIS) Project, ASTI Building, C.P. Garcia Avenue, Diliman, Quezon City, Philippines – (johnbartlovern.dumalag, karllouie.mariano, neyzielle.cadiz, ning)@asti.dost.gov.ph, (jcfaceron, maiafelicen, mcgelido)@gmail.com
[2] DOST Advanced Science and Technology Institute, ASTI Building, C.P. Garcia Avenue, Diliman, Quezon City, Philippines

KEY WORDS: Remote Sensing, Radar, S-band SAR, Flood Mapping, Disaster Response

ABSTRACT:

The Philippines' Advanced Science and Technology Institute under the Department of Science and Technology (DOST-ASTI) has developed an AI-based and near real-time flood extent mapping service that utilizes C-Band Sentinel-1 SAR images. However, this method is limited by the availability of the Sentinel-1 images during flooding events. To address this issue, the institute, through its SARwAIS Project, utilized the S-Band NovaSAR-1 satellite, which was designed and launched by Surrey Satellite Technology, Ltd. With a 10% share to NovaSAR-1's imaging capacity, the country can task image acquisitions that could help augment the Sentinel-1 datasets. Successfully captured images are prepared using the institute's developed pre-processing workflow. Afterwards, a thresholding method, adopted from UN-SPIDER's recommended practices for flood mapping, is employed to identify potentially flooded areas from these images. Generated products are then assessed to determine their relative accuracy in detecting potential floods. Satisfactory products are then distributed to relevant disaster management agencies and are also published in the agency's social media page for further information dissemination. Python scripts were then developed to automate the established workflows, which were initially done manually. These scripts also help expedite the generation of flood maps especially when processing multiple SAR images. The acquisition and utilization of NovaSAR-1 images substantially help the country address the gaps on the availability of workable data for a more informative disaster response especially during flooding events.

1. INTRODUCTION

1.1 Background of the Study

Flooding is a recurring issue in the Philippines due to the frequent occurrence of tropical cyclones and other severe weather disturbances. To facilitate quicker and more informed responses to such events, an AI-driven method for mapping potential flood areas was developed in 2020. This methodology relies on historical Sentinel-1 (S1) SAR images and an AI model to estimate potential flood extents during severe weather incidents in the country. Since its development and implementation, this workflow has been used to produce potential flood extent maps whenever S1 SAR data is accessible (de la Cruz et al., 2020). These maps are subsequently distributed to government agencies responsible for disaster response operations.

Prior to December 2021, both Sentinel-1A and 1B (S1-A and S1-B) had the potential to capture SAR images over a specific area every 6 days, as noted by the (ESA, 2022). This relatively frequent revisit schedule provided ample opportunities for obtaining SAR images for the creation of near-real-time flood extent maps. However, following the failure of the S1-B satellite in December 2021, the acquisition of S1 SAR images now occurs only every 12 days. Consequently, there are fewer chances to acquire S1 SAR images over regions experiencing severe weather events. This limitation also means that the AI-based method, which relies exclusively on S1 SAR images, is less likely to be utilized for generating flood situation maps for affected areas. This issue significantly reduces the country's capacity to promptly generate and provide flood maps to relevant agencies, thus potentially hindering their ability to respond swiftly and effectively. There are also instances where estimated flood extent maps cannot be produced due to the insufficient availability of S1 SAR images for processing.

1.2 Objectives

The constraint of AI-based flood mapping emphasizes the necessity of incorporating alternative SAR products to enhance the current operational process for creating near-real-time flood situation maps. This paper discusses the integration of S-Band NovaSAR-1 images into the flood extent mapping service of DOST-ASTI. Furthermore, it outlines the established and implemented operational workflow for generating potential flood maps using these images. The paper also examines the limitations associated with the use of NovaSAR-1 images in the context of potential flood mapping activities.

2. REVIEW OF RELATED LITERATURE

In synthetic aperture radar (SAR) images, there is generally a good contrast between water and non-water features, as the former typically exhibit much lower backscatter values compared to the latter (Rahman & Thakur, 2018). This phenomenon arises from the specular reflection of the SAR signal on the water's surface (Richards, 2009; Scotti et al., 2020). This distinctive radar signal response over water bodies has been employed in various processes, including supervised and unsupervised classification, thresholding techniques, and artificial intelligence-based methods, to aid in the identification of potential flood extents, particularly in open areas (Iglesias et al., 2018; Rahman & Thakur, 2018; de la Cruz R. et al, 2020). Specifically, areas potentially affected by flooding are expected to show reduced or diminished backscatter values due to the presence of water, resulting in a relatively darker appearance.

* Corresponding author

2.1 AI Flood Mapping in the Philippines

In the Philippines, DOST-ASTI developed an automated flood mapping system based on Artificial Intelligence in 2020, achieving a detection accuracy of 90% (de la Cruz et al., 2020). This system utilizes Sentinel-1 SAR images with VH polarization to rapidly provide information on the extent of flooding to government agencies. Specifically, a false color composite image is created by combining two images captured during dry periods before the flooding incident with an image taken during the flooding event. In this composite image, potentially flooded regions are emphasized and appear in cyan. An artificial intelligence model is subsequently employed to swiftly identify these pixels or areas that are potentially flooded. Nevertheless, the efficiency of this approach is somewhat limited by the accessibility of Sentinel-1 SAR images, especially during severe weather events that may result in flooding.

Previously, S1-A and S1-B could potentially capture new images over a specific area every six days. However, on December 2021, S1-B malfunctioned, and was eventually deemed as inoperable (ESA, 2022). This failure of S1-B resulted in new S1 SAR images being captured only by S1-A satellite every 12 days. This relatively longer return for capturing new images means that there could be more instances when there will be no available S1 SAR images during flood events. This gap in the availability of datasets for the generation of potential flood extent maps can be addressed by utilizing the NovaSAR-1 images.

2.2 NovaSAR-1 Satellite

NovaSAR-1 is a low-cost, S-band SAR satellite that was developed and launched last September 2018 by Surrey Satellite Technology LTD or SSTL, a UK-based company, and Airbus DS, in collaboration with partner organizations from India, Australia, and Philippines (DOST-ASTI, 2021, CSIRO, 2022). The Philippines, through DOST-ASTI's Synthetic Aperture Radar and Automatic Identification System for Innovative Terrestrial Monitoring and Maritime Surveillance (SARwAIS) Project, has acquired a 10% imaging capacity on the NovaSAR-1 satellite (Vicente et al., 2020). This translates to approximately 180 seconds of imaging control per day, which is then used to acquire SAR images anywhere in the country, including its maritime domain.

The NovaSAR-1 satellite can acquire SAR images in Stripmap and ScanSAR modes (CSIRO, 2020). Stripmap mode has a ground resolution of approximately 6 meters. For ScanSAR mode, several ground resolutions can be set, but 20-meter resolution is regularly acquired. In terms of polarization, most image acquisitions can only be set to either HH or VV polarization only. However, there are instances when some acquisitions can be set to have two (HH, HV) to three (HH, HV, VV) polarizations.

Acquisitions of NovaSAR-1 images over the same area is estimated to be every 16 days. However, this return period can potentially be lowered as the acquisition parameters of the satellite like the incidence angle and look direction (left or right-side look) can be modified. This means that this satellite can acquire new images over the same area within a shorter period, albeit the acquisition parameters of the two images will already be different.

One issue with NovaSAR-1 images acquisitions is its orbit drifts westward during each repeat cycle. This means that new images with similar acquisition parameters and are acquired over a specific area are expected to be shifted to the west (CSIRO, 2020). This implies that any analyses that use historical SAR images of an area (e.g., interferometry, possibly some change detection) is not readily doable since their orbital parameters are already significantly different.

Based on the stated characteristics of NovaSAR-1 images and its acquisition parameters, it can be implied that these images can be used to map potential flood extents. However, it should be noted that the AI method is currently not a viable option since this method requires consistent SAR image acquisition parameters, which is not possible with NovaSAR-1 primarily due to its orbital shift (CSIRO, 2020, de la Cruz et al., 2020). This means that alternative ways to generate potential flood maps from NovaSAR-1 images must be explored and employed.

2.3 Threshold Method of Flood Mapping

One of the simplest ways to do identify potential flood extents from SAR images is through the thresholding method (Iglesias et al., 2018; Rahman & Thakur, 2018; Liang & Liu, 2019). In this method, the threshold value to be used is manually identified. This value is assumed to be the boundary between water and non-water pixels and is applied to the SAR image to rapidly classify the pixels as either water or non-water. Since water bodies are expected to have lower backscatter values, any pixels whose values are lower than the threshold value are reclassified as water pixels. Then any pixels whose values are higher than the threshold value are reclassified as non-water pixels.

A threshold value can be determined through trial and error wherein certain values are applied to the image and the ones that are deemed to yield the best output is considered the final threshold value. Another way is through the simple analysis of the histogram of the backscatter values of the image (Iglesias et al., 2018; UN-SPIDER, 2020). Generally, the histogram of SAR images that cover water and non-water bodies is assumed to have a bimodal distribution, i.e., it shows two peaks. The peak with the lower intensity values corresponds to the water bodies, while the other peak corresponds to the non-water bodies. The threshold value is then reckoned to be located at the lowest points between the two peaks (Liang & Liu, 2019; UN-SPIDER, 2020). These methods are the simplest and fastest ways to determine a threshold value and they do not require special image processing or analyses.

One limitation of the threshold method is the applicability of the identified threshold value. A threshold value may yield fairly good results when applied to a certain SAR image scene, but it may yield erroneous output when used on another SAR image scene that was acquired at a different area (Tan, 2004; de la Cruz, 2020). This means that different threshold values may be required for different SAR image scenes to ensure relatively good results.

Another limitation of thresholding method is it cannot readily filter out false positives due to inland waters and terrain effects, something that the AI-based method can do. Nevertheless, these false positives can be removed by applying masks specifically for these features (Rahman & Thakur, 2018).

The UN Office for Outer Space Affairs or UN OOSA's UN-SPIDER, shows in their Recommended Practices for radar-based flood mapping a process workflow for rapid flood mapping based on thresholding method (UN-SPIDER, 2020). While their workflow uses Sentinel-1 SAR satellites in the generation of their

outputs, the concepts behind it can still be used in the generation potential flood extent maps from NovaSAR-1 images.

3. METHODOLOGY

In the developed workflow, flood mapping through thresholding of NovaSAR-1 images is employed. Specifically, the SARwAIS team adopted the concepts behind the UN-SPIDER's workflow and applied them to NovaSAR-1 images.

3.1 General Workflow

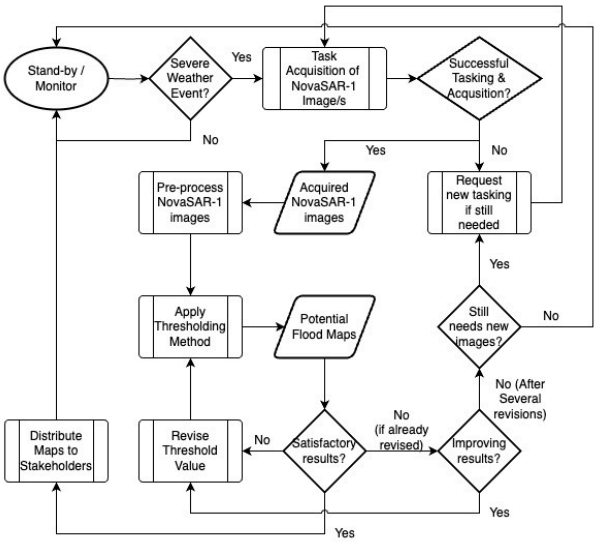

Figure 1. General workflow employed by DOST-ASTI's SARwAIS team in using NovaSAR-1 images for rapid flood mapping during extreme weather events.

During occurrences of severe weather events brought about by tropical cyclones, the SARwAIS team initially determines the availability of the NovaSAR-1 images on affected regions. If NovaSAR-1 image acquisition is possible, a tasking request is sent to SSTL for possible upload to the satellite. If the tasking and image acquisition is successful, SSTL downloads the captured NovaSAR-1 image/s through their ground receiving stations, and subsequently processes these into Level-1 products, which they will then transfer to DOST-ASTI. Once received, these images are then pre-processed using the project's established pre-processing workflow to generate analysis-ready, Level-2 products in GeoTiff format. Afterwards, thresholding method is applied to the pre-processed image to generate the maps. Outputs are then checked by remote sensing specialists in the team. Once cleared and considered to have adequately captured the flooding event/s, they are then distributed to stakeholders, disaster actors, as well as local government unit officials of the affected communities. The recipient of these maps includes the Office of Civil Defense (OCD), the National Disaster Risk Reduction and Management Council (NDRRMC), and some are coursed through the DOST's regional offices. The details of the pre-processing workflow and thresholding method applied to the images are discussed in the succeeding sections. Figure 1 shows the general workflow that DOST-ASTI employs.

3.2 Data Processing

Before doing any analysis on SAR images, it is important to ensure that they are pre-processed into analyses-ready, level 2 products. This means the SAR image must be properly calibrated, geometrically corrected, and already in the appropriate map projection.

3.2.1 NovaSAR-1 Pre-processing. For flood mapping applications, 20m ScanSAR images of HH polarization are tasked for acquisition. If the tasking and acquisition is successful, the raw data are subsequently processed by SSTL into a Level 1 SCD product. This is a multi-looked, ground range detected product that is already radiometrically calibrated into sigma0 (CSIRO, 2020).

The pixel values of SCD products are the estimated amplitude values of the detected signal. Calibration constant K, found in the images' metadata, is applied to the image to convert the pixel integer value into the correct scaled intensity value. Equation 1 below shows the equation used in applying the calibration constant to the NovaSAR-1 image (CSIRO, 2020).

$$Scaled\ intensity = \frac{(Pixel\ Amplitude)^2}{K} \quad (1)$$

This product is then pre-processed to remove the geometric distortions inherent to SAR images and apply correct map coordinates to each pixel. The intensity values were also converted into their equivalent decibel scale values.

The pre-processing of a NovaSAR-1 image is done using the SNAP 8 software with version 1.2.2 of the NovaSAR-1 product reader plug-in installed. This version of the plug-in ensures that NovaSAR-1 images are read properly, and pre-processing functions of SNAP for these images will yield good outputs (Cohen, 2022). The SNAP 8 software used is installed in one of the virtual machines in DOST-ASTI COARE's High Performance Computing (HPC) facility, which runs a Linux OS. This virtual machine has 88 cores, and around 504 GB of RAM, which is enough to readily process full scenes of NovaSAR-1 images that can be several gigabytes in size.

The general pre-processing workflow applied to NovaSAR-1 images is shown in Figures 2 and 3. The Apply Calibration Constant step implements the equation shown in Equation 1 using the Band Math tool. The SAR-Mosaic shown in Figure 2a is used to apply map coordinates to the SAR image without any geometric distortion correction. Terrain Correction step shown in Figure 2b runs the Terrain-Correction (TC) tool, which removes the geometric distortion in the SAR image, and applies the desired map coordinates. Prior to the release of version 1.2.2 of the NovaSAR-1 plug-in, the TC tool was found to yield problematic outputs, hence the SAR-Mosaic step was initially used. Lastly, the Conversion to Decibels step runs the LinearToFromdB tool, which converts the pixel values into decibel scale. The final output of these steps are terrain corrected products projected into the WGS-84 coordinate system stored in the Geo-Tiff format.

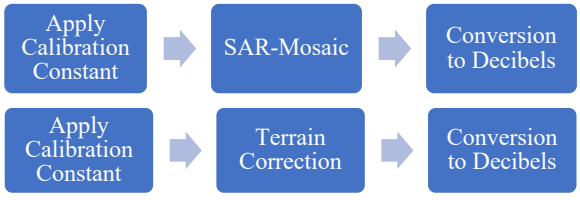

Figure 2. General preprocessing workflow for NovaSAR-1 images.

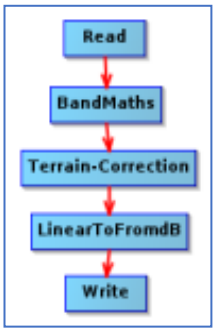

Figure 3. Preprocessing workflow as shown in the Graph Builder tool in SNAP.

3.2.2 Flood Detection. To rapidly identify the potentially flooded areas from the pre-processed NovaSAR-1 images, the thresholding method is employed. Specifically, the determination of threshold values and the binarization process based on the workflow of UN-SPIDER was adopted. Furthermore, the processes after the binarization step from the workflow of the AI based flood mapping were adopted as well.

The employed workflow was initially implemented using available GIS processing tools in QGIS 2.14. This version of QGIS is the only one installed in the same virtual machine used to pre-process the images. The new workflow is summarized in Figure 4 below.

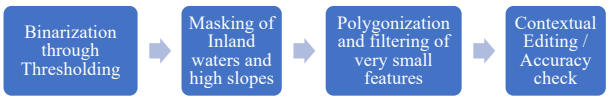

Figure 4. Summary of the workflow for flood mapping using thresholding method

3.2.2.1 Binarization through thresholding. The threshold value to be used is initially identified by analyzing the histogram of the SAR image being processed. If the histogram of this image has a bimodal distribution, the threshold value is chosen from the lowest values between the two peaks. However, if the histogram does not exhibit a bimodal distribution or the results based on the identified threshold value are unsatisfactory, then new threshold value are identified by checking the value of the pixel that lies within the visually apparent boundary between the water and non-water areas.

If a threshold value Th is already identified, the SAR image is then binarized using this value. To do this, the raster calculator tool is used. Equation 2 shows the expression used to binarize the image.

$$(pixel \leq Th) * 1 + (pixel > Th) * 0 \qquad (2)$$

This expression means that any pixels with values less than or equal to the threshold value will be assign with a value of 1, which corresponds to water pixels or potential floods. Otherwise, the pixel will be assigned a value of 0, which then corresponds to non-water pixels. The output of this step is a raster showing the binarization or reclassification of the input SAR image.

3.2.2.2 Masking of inland waters and high slopes. The binarized SAR image is expected to contain false positives due to the presence of permanent inland waters and low backscatter values due to terrain or possibly noise inherent to the acquisition of the image (Rahman & Thakur, 2018). To remove these potential false positives, a mask for removing the inland waters and high slope areas is applied. The mask used in this step is based on the same mask developed for the AI-based method. Equation 3 shows the expression used to implement this in raster calculator.

$$(binarized\ raster) * (mask\ raster) \qquad (3)$$

It should be noted that the applied mask is a raster file containing DN values of only 1, which corresponds to pixels that can be flooded, and 0 or pixels that cannot be flooded.

3.2.2.3 Polygonization and filtering very small features. In this step, the masked raster file is converted into a vector format (i.e., shapefile), wherein each feature has attribute values of either 1 or 0 only. Afterwards, the area of each feature is calculated, and any feature that are greater than 3,000 square meters are retained, while the rest are deleted. Filtering of relatively small features assumes that any features smaller than the specified area are potentially noise only.

3.2.2.4 Contextual editing / Accuracy Check. In this step, a final contextual editing is done wherein the output is checked in a GIS software like QGIS for any remaining potential erroneous classifications that should be removed. This step involves the radar remote sensing expertise of staff assigned to check the outputs, as well as his familiarity with the area covered by the processed image.

Furthermore, a visual comparison between the outputs and the source image is done. If the comparison indicates that the results is unable to capture substantial areas of potentially inundated areas, then a new threshold value must be determined, and the image reprocessed using this new value. This process is usually repeated until the results are deemed to satisfactorily capture most of the potentially flooded areas. However, in case no satisfactory outputs are generated after several iterations, then the team may opt to request for new images to be acquired and processed, thereby doing the same processes as discussed.

3.2.3 Automating the Workflows. Python scripts were created to automate the pre-processing and thresholding workflows. Specifically, the script for pre-processing NovaSAR-1 image can automatically extract necessary information from the image's metadata and then apply the workflow shown in Figure 2. On the other hand, the script for the thresholding method automatically executes the workflow shown in Figure 3, provided that the threshold value to be used has been manually identified prior to processing.

This automation also includes provisions for batch pre-processing of several NovaSAR-1 images, and generation of the shapefiles for potential floods from each image. These scripts ensured that this workflow is operationalized with minimal human intervention as they only require the filenames of the input images, and the threshold to be applied.

4. RESULTS AND DISCUSSIONS

4.1 Image Acquisition to Map Generation

Successfully acquired images are downloaded from the satellite, processed into level 1 products, and then sent to DOST-ASTI typically in less than 24 hours after acquisition. Level-1 NovaSAR-1 products are provided in strip format, which leads to

extended pre-processing durations. The pre-processing stage, where the image is transformed into a Level-2 product, typically requires an hour or more, with the exact timeframe depending on the image's size. Once the Level-1 product is generated, the flood extents are extracted. This process previously takes a few more hours especially when it was still done manually. Eventually, this has significantly improved with the creation of the processing scripts. When processes run seamlessly, flood maps can typically be prepared for distribution within a day following the image acquisition. While this latency is relatively long, the generated and distributed maps can still be useful to the recipients of these maps.

4.2 Generated Flood Maps

Since 2020, the SARwAIS team has successfully generated potential flood maps using NovaSAR maps for the several severe weather disturbances that has affected the country. There are several instances when the NovaSAR-1 images were able to compliment and augment the Sentinel-1 datasets by covering areas that do not have any available Sentinel-1 images. Because of this, the team was still able to generate flood impact maps distributed stakeholders via email, encouraging them to use the maps as they see fit for the disaster response efforts. Many of the generated maps have also been distributed to agencies and institutions in addition to the maps generated through the AI method, which uses Sentinel-1 datasets. Some of these maps were also posted in the DOST-ASTI's social media accounts for public access and further distribution. The files being distributed are in the form of maps layouts as well as shapefiles.

Table 1 shows several instances when NovaSAR-1 images were used to generate flood maps during severe weather events that affected the country. It also shows the events where flood maps were generated and subsequently distributed to the relevant stakeholders and intended local government units. It also shows that there are instances when images were processed but the generated maps were not distributed. This happens when there is a substantial delay in the receipt of the acquired images from SSTL or in the processing of the datasets. In both instances, the generated maps become obsolete and no longer used for distribution.

Tropical Cyclone (local name) / Weather Event	NovaSAR-1 Date	Map from NV1 distributed to stakeholders?	With Sentinel-1 data a few days before / after?
Ulysses	13-Nov-20	Yes	Yes
Dante	02-Jun-21	No	Yes
Fabian	22-Jul-21	Yes	Yes
Jolina	08-Sep-21	Yes	Yes
Maring	11-Oct-21	Yes	Yes
Odette	15-Dec-21	No	Yes
Florita	25-Aug-22	Yes	Yes
Paeng	30-Oct-22	Yes	Yes
Severe rains	Jan-23	No	Yes
Severe rains	Aug-23	No	Yes

Table 1. Summary of several instances when NovaSAR-1 images were used to generate flood maps during severe weather events that affected the country.

Figures 5 to 8 shows samples outputs for flood mapping using NovaSAR-1 datasets. Figure 5 shows a NovaSAR-1 image overlayed on a Google Satellite Base map. The potentially flooded areas are also highlighted in orange color. NovaSAR-1 images are typically processed and distributed as strips like the image shown in Figure 5. Figure 6 shows the overlay of potential flood extents for NovaSAR-1 image (oranges features) and the overlay of features generated from Sentinel-1 image. Both images were acquired on the same date and is separated only by a few hours. The difference in the apparent extents of their detected potential floods is likely due to the difference in the wavelength, of the signal being used by the two systems. The S-band signal of NovaSAR-1 can penetrate the vegetation canopy more than the C-band sign. Hence, it can detect, to some extent, the flooding underneath the vegetation.

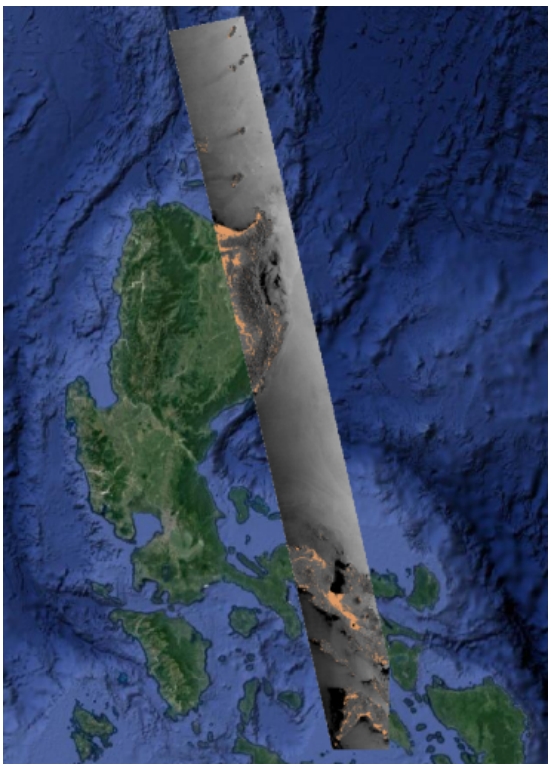

Figure 5. A sample NovaSAR-1 image acquired for the Typhoon Ulysses last November 2020. The detected potential flood extents are shown in orange color. This output is one of the initial attempts to use NovaSAR-1 for flood mapping.

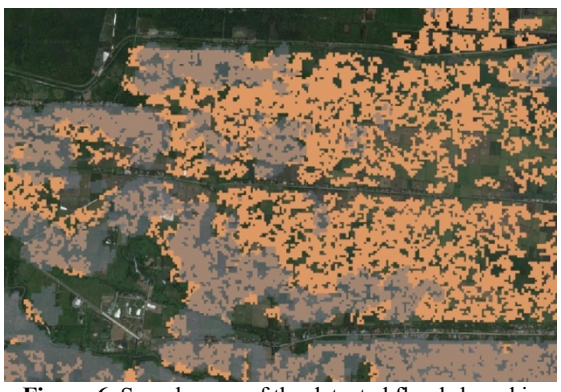

Figure 6. Sample over of the detected floods based in NovaSAR-1 (orange features) and Sentinel-1 image (light brown features). The NovaSAR-1 image used for this output is the one shown in Figure 5.

Meanwhile, Figure 7 shows two maps indicating the general extent of the acquired images, and the corresponding footprint of the generated map layouts which were subsequently distributed and cascaded to the public. Figure 7 provides an example on how NovaSAR-1 was used the cover the areas with no available Sentinel-1 acquisitions during an on-going severe weather event. Lastly, Figure 8 shows an example of a map derived from a

NovaSAR-1 image that was acquired during the onslaught of tropical cyclone Fabian (international name In-Fa) last July 2021. This is the typical maps layout generated by DOST-ASTI. These maps are automatically generated using scripts running in a QGIS software.

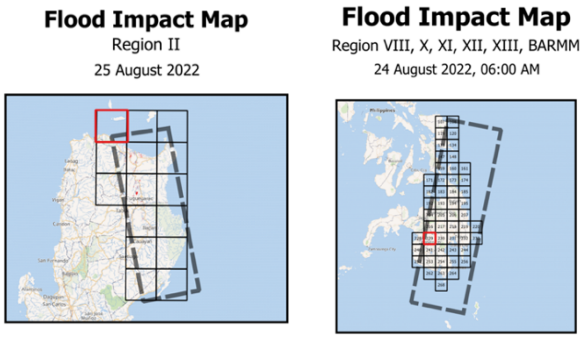

Figure 7. Sample map showing the areas where flood maps were generated from NovaSAR-1 (left) and Sentine-1 (right) images for tropical storm Florita last August 2022. Note the different acquisition dates of the two images.

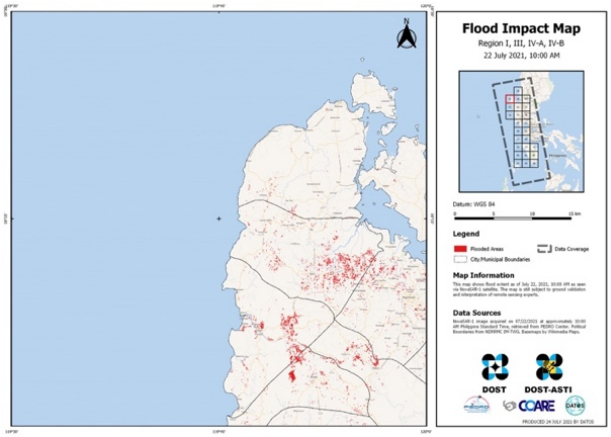

Figure 8. Sample map generated for tropical cyclone Fabian last July 2021. This kind of map is generated and distributed to the stakeholders. The same map layout template is used for maps generated from Sentinel-1 images.

4.3 Challenges with Flood Mapping Using NovaSAR-1

4.3.1 Tasking and Timeliness of images. Unforeseen situations may arise where the acquisition of images does not proceed as initially planned. This can occur due to conflicts with imaging requests from other collaborating organizations, particularly when the specified imaging timeframe is tight, often spanning just a few days. Failures in tasking can also occur due to clashes with the satellite's pre-scheduled downtime or unexpected operation interruptions. These tasking failures consequently results in lost opportunities to generate potential flood maps that could have potentially been useful to the relevant agencies and intended recipients. To address this challenge, the institute submits a new tasking request, particularly when the circumstances make it necessary to do so.

Sometimes, there are also delays in obtaining the requested images that DOST-ASTI has requested for capture. These delays can extend to several days, rendering the information on flood extents derived from these images almost obsolete as it no longer offers near-real-time data on the flooding situation. In response to this challenge, DOST-ASTI has embarked on the integration of the satellite into its own ground receiving station. This integration enables the agency researchers to directly download the images it has requested and automatically process them into the required products for various established operations and services, including flood mapping.

4.3.2 Determining a Good Threshold Value. Obtaining an optimal threshold value poses a significant challenge in the creation of flood maps from NovaSAR-1 images. This challenge primarily arises from the inherent characteristics of NovaSAR images, wherein bodies of water, particularly those situated in the near-range aspect, exhibit a bright appearance rather than the expected dark appearance. This can be attributed to the incidence angle of 24.5-28.9° that is typically used in the acquisition of these images. These values are relatively low compared to other SAR systems like Sentinel-1 and can yield brighter pixels that are indicative of high backscatter values (ESA, 2007).

Due to the apparent brightness of water bodies of NovaSAR-1 images, their histograms generally have unimodal distribution instead of bimodal, which in turn makes it difficult to determine the appropriate threshold value. Whenever this happens, the only option is to iterate on several test threshold values and check which one yield the best and satisfactory flood extent maps. Figure 9 shows an example of a NovaSAR-1 image captured to determine extents of potential flood maps during the onslaught of Tropical Storm Nalgae. Figure 10 shows the sample unimodal histogram of the SAR image shown in Figure 9.

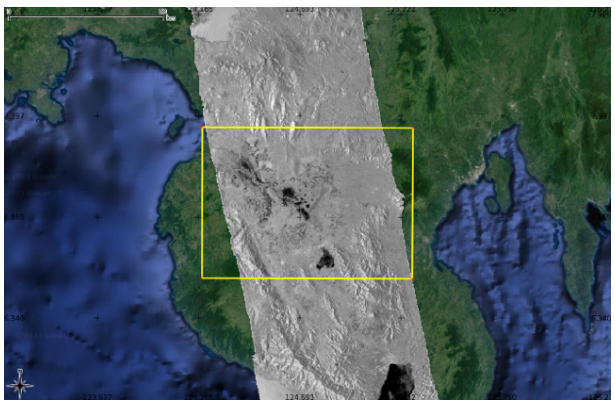

Figure 9. Sample pre-processed NovaSAR-1 20m ScanSAR image that was acquired for a severe weather event last October 2022.

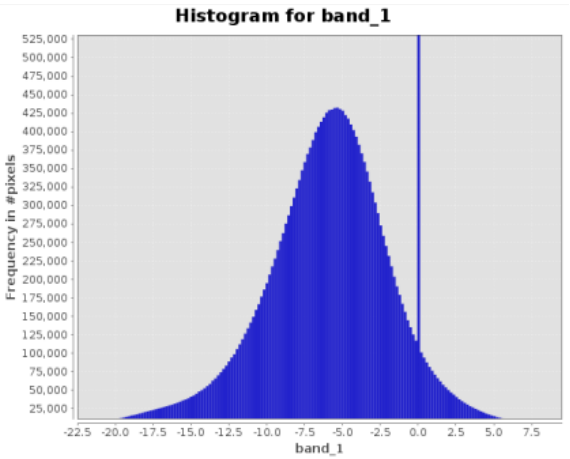

Figure 10. Histogram of the sample NovaSAR-1 20m ScanSAR image shown in Figure 5. The apparent high frequency of pixels with zero value is due to the assignment of NaN pixels with zero.

4.3.3 Accuracy and Validation. Before disseminating the generated maps to the intended agencies and offices, a thorough examination is carried out by the remote sensing experts within the SARwAIS team. This examination is vital to guarantee the maps' precision in delineating potential flood extents. In cases where the employed threshold value produces an excessive number of false positives or false negatives, the team will initiate the replacement of the threshold value and proceed to generate new potential flood maps.

Upon achieving satisfactory results with the newly adjusted threshold, the maps undergo a final evaluation and contextual editing process. During this phase, the outputs are scrutinized, and any seemingly erroneous detections are removed from the dataset.

Considering the critical and time-sensitive nature of the generated products, the team's leader typically grants authorization for their distribution without the customary accuracy assessment, such as the creation of an error matrix. This is specifically and occasionally done if the products were generated within an acceptable timeframe to ensure their relevance and prevent them from becoming obsolete. The recipients of the generated products are informed about this concern through disclaimers and are encouraged to provide feedback on the accuracy of the flood maps that they have received.

While it is anticipated that these maps may contain misclassifications or false positives, the distributed maps are deemed to be of significant accuracy and remain highly valuable within the framework of an informed response to flooding events. Furthermore, the primary objective of generating these maps is to provide near-real-time information concerning the approximate extent and impact of flooding in the affected regions. It is important to note that there is a lack of readily available field validation data that can be used to precisely determine the actual accuracy of these maps. Hence, the usual remote sensing requirement of error matrix computation is generally no longer done every time a flood map is generated.

4.3.4 Manual Processing. During the initial applications of NovaSAR-1 for mapping potential map extents, the processes used to generate the flood maps were done manually using the built-in tools of a QGIS software installed in the virtual machines used to process these images. This proved to be tedious and very prone to errors, which may require repetition of the executed processes to rectify any mistakes made. This can become even more problematic especially if the applied threshold value did not yield satisfactory outputs as the entire process has to be repeated. When this happens, the information from the images that are being processed slowly become obsolete.

To address this issue, the team developed a processing script based on Python. This script serves as an automation tool, streamlining the entire flood map generation process through thresholding, thus enhancing efficiency and speed. The user-friendly script necessitates only specifying the files to be processed and the associated threshold values. Moreover, it is versatile enough to handle multiple images, contingent on the user's input of the requisite information. Notably, the script has been designed to process not only NovaSAR-1 images but also various other SAR images.

5. CONCLUSION

DOST-ASTI has effectively incorporated S-Band NovaSAR-1 images into its flood extent mapping service. With this integration, an operational workflow for the creation of potential flood maps using NovaSAR-1 images has been meticulously established and is now fully operational. This workflow is automated, ensuring expedited and simplified flood map generation during instances of severe weather events, provided that the images are successfully acquired.

While the utilization of NovaSAR-1 images for flood extent mapping has presented its share of challenges, the successful generation of flood maps from NovaSAR-1 images on numerous occasions—irrespective of Sentinel-1 dataset availability—and their subsequent dissemination to diverse stakeholders underscore the capacity of these images to effectively complement the latter in the production of near-real-time flood extent maps.

ACKNOWLEDGEMENT

This paper is made possible through the Synthetic Aperture Radar and Automatic Identification System for Innovative Terrestrial Monitoring and Maritime Surveillance (SARwAIS), a Research and Development Project funded by the Department of Science and Technology and the Philippine Council for Industry, Energy and Emerging Technology Research and Development (DOST-PCIEERD), implemented by the Advanced Science and Technology Institute (DOST-ASTI).

REFERENCES

Cohen, M., 2022: SNAP NovaSAR Product Reader, SNAP software plug-in version 1.2.2, Brockmann Consult GmbH, SNAP Community Plug-ins, https://github.com/bcdev/snap-novasar-reader (2022)

CSIRO, 2020: NovaSAR-1 User Guide. *CSIRO Centre for Earth Observation*, research.csiro.au/cceo/novasar/novasar-introduction/novasar-1-user-guide/

de la Cruz, R. M., Olfindo Jr., N. T., Felicen, M. M., Borlongan, N. J. B., Difuntorum, J. K. L., Marciano Jr., J. J. S., 2020: Near-Realtime Flood Detection from Multi-Temporal Sentinel Radar Images Using Artificial Intelligence. *The International Archives of the Photogrammetry, Remote Sensing and Spatial Information Sciences*, vol. XLIII-B3-2020, 2020, pp. 1663–1670, https://doi.org/10.5194/isprs-archives-XLIII-B3-2020-1663-2020.

DOST-ASTI 2019: DOST-ASTI, SSTL Sign Capacity-sharing Agreement for NovaSAR-1 satellite. *DOST-ASTI,* https://asti.dost.gov.ph/communications/news-articles/dost-asti-sstl-sign-capacity-sharing-agreement-for-novasar-1-satellite/

DOST-ASTI, 2021: DOST SIYASAT Portal - NovaSAR Data for Actionable Insights. *DOST SIYASAT Portal*. siyasat.asti.dost.gov.ph/icps/aboutnovasar.

DOST-ASTI, 2022: SARwAIS Project Holds 2nd Stakeholders Meeting. *Department of Science and Technology – Advanced Science and Technology Institute,* https://asti.dost.gov.ph/resources/media-release/sarwais-project-holds-2nd-stakeholders-meeting/

ESA, 2007: ASAR Product Handbook. *European Space Agency* , earth.esa.int/eogateway/documents/20142/37627/ASAR-Product-Handbook.pdf

ESA, 2022: Mission Ends for Copernicus Sentinel-1B Satellite. *European Space Agency*, www.esa.int/Applications/Observing_the_Earth/Copernicus/Sentinel-1/Mission_ends_for_Copernicus_Sentinel-1B_satellite

Iglesias, R., Garcia-Boadas, E., Vicente-Guijalba, F., Centolanza, G., Duro, J., 2018: Towards Unsupervised Flood Mapping Generation Using Automatic Thresholding and Classification Aproaches. *IGARSS 2018 - 2018 IEEE International Geoscience and Remote Sensing Symposium.* doi:10.1109/igarss.2018.8519111

Liang, J., Liu, D., 2020: A local thresholding approach to flood water delineation using Sentinel-1 SAR imagery. *ISPRS Journal of Photogrammetry and Remote Sensing, 159, 53–62.* DOI: 10.1016/j.isprsjprs.2019.10.017

Rahman, Md.R., Thakur, P. K., 2018: Detecting, Mapping and Analysing of Flood Water Propagation Using Synthetic Aperture Radar (SAR) Satellite Data and GIS: A Case Study from the Kendrapara District of Orissa State of India. *The Egyptian Journal of Remote Sensing and Space Science* 21 (July): S37–41. https://doi.org/10.1016/j.ejrs.2017.10.002.

Richards, J.A., 2009: *Remote Sensing with Imaging Radar. Signals and Communication Technology*, Berlin, Heidelberg, Springer Berlin Heidelberg

Scotti, V., Giannini, M., Cioffi, F., 2020: Enhanced Flood Mapping Using Synthetic Aperture Radar (SAR) Images, Hydraulic Modelling, and Social Media: A Case Study of Hurricane Harvey (Houston, TX). *Journal of Flood Risk Management*, July. https://doi.org/10.1111/jfr3.12647.

Tan, Q., Bi, S.W., Hu, J.P., Liu, Z.J., 2004: Measuring Lake Water Level Using Multi-Source Remote Sensing Images Combined with Hydrological Statistical Data. *IEEE International Geoscience and Remote Sensing Symposium* 2004, https://doi.org/10.1109/igarss.2004.1370258.

UN-OOSA, 2020: Step by Step: Recommended Practice Flood Mapping | UN-SPIDER Knowledge Portal. *United Nations Office for Outer Space Affairs*, www.un-spider.org/advisory-support/recommended-practices/recommended-practice-flood-mapping/step-by-step

Vicente, R., Tabanggay, L., Rayo, J., Mina, K., Retamar, A., 2020: Earth Observation Applications for Goal 14: Improving Maritime Domain Awareness Using Synthetic Aperture Radar Imaging with Automatic Identification System in the Philippines. *The International Archives of the Photogrammetry, Remote Sensing and Spatial Information Sciences* XLIII-B3-2020 (August): 215–19. https://doi.org/10.5194/isprs-archives-xliii-b3-2020-215-2020.